Table 2. *Distances* (Å) *and angles* (°) *in the* MoO_6 *and* PO_4 *polyhedra and main* Tl—O *distances*

The Mo—O^{i} or P—O^{i} distances are on the diagonal, above it are the O^{i}—O^{j} distances and under it are the O^{i}—Mo—O^{j} angles.

Mo(1)	O(1)	O(2)	O(3)	O(4)	O(5)	O(6)
O(1)	1·66 (1)	2·68 (2)	2·74 (2)	2·83 (2)	2·74 (2)	3·81 (2)
O(2)	92·9 (7)	2·01 (2)	2·41 (2)	2·77 (2)	2·92 (2)	2·80 (2)
O(3)	96·3 (7)	168·8 (6)	2·00 (1)	2·78 (1)	2·92 (2)	2·86 (2)
O(4)	98·5 (6)	85·8 (6)	86·5 (5)	2·06 (1)	4·06 (2)	2·83 (2)
O(5)	95·2 (6)	92·7 (6)	92·9 (6)	166·2 (5)	2·02 (1)	2·74 (2)
O(6)	175·8 (6)	84·3 (6)	86·9 (6)	84·4 (6)	81·9 (6)	2·15 (2)

Mo(2)	O(7)	O(8)	O(9)	O(10)	O(11)	O(12)
O(7)	1·66 (1)	2·73 (2)	2·81 (2)	2·82 (2)	2·70 (2)	3·83 (2)
O(8)	93·9 (7)	2·05 (2)	2·46 (2)	2·84 (2)	2·87 (2)	2·74 (2)
O(9)	99·5 (7)	166·6 (7)	2·00 (2)	2·78 (2)	2·84 (2)	2·85 (2)
O(10)	100·8 (7)	89·2 (6)	88·5 (6)	1·99 (1)	3·99 (2)	2·73 (2)
O(11)	93·4 (6)	89·5 (6)	89·5 (6)	165·8 (6)	2·03 (1)	2·82 (2)
O(12)	174·0 (7)	80·7 (6)	86·0 (6)	81·7 (6)	84·1 (5)	2·18 (1)

P(1)	O(6^{i})	O(8^{ii})	O(9^{iii})	O(13)
O(6^{i})	1·52 (2)	2·57 (2)	2·55 (2)	2·52 (2)
O(8^{ii})	115·9 (9)	1·52 (2)	2·46 (2)	2·53 (2)
O(9^{iii})	113·3 (9)	107·1 (9)	1·54 (2)	2·48 (2)
O(13)	107·5 (8)	108·1 (9)	104·2 (8)	1·61 (1)

P(2)	O(4^{iv})	O(11)	O(12^{ii})	O(13)
O(6^{iv})	1·52 (1)	2·47 (2)	2·48 (2)	2·45 (2)
O(11)	109·9 (8)	1·50 (1)	2·53 (2)	2·48 (2)
O(12^{ii})	111·6 (8)	116·3 (9)	1·48 (2)	2·51 (2)
O(13)	103·5 (8)	106·2 (8)	108·5 (8)	1·60 (2)

P(3)	O(2^{v})	O(3^{iv})	O(5)	O(10^{vi})
O(2^{v})	1·54 (2)	2·41 (2)	2·54 (2)	2·48 (2)
O(3^{iv})	103·8 (8)	1·51 (2)	2·53 (2)	2·44 (2)
O(5)	111·9 (9)	113·3 (8)	1·52 (2)	2·49 (2)
O(10^{vi})	108·9 (9)	107·9 (9)	110·7 (8)	1·50 (2)

Tl(1)—O(2^{vii})	3·07 (2)	Tl(1)—O(13^{iv})	3·57 (2)
Tl(1)—O(2)	3·00 (2)	Tl(2)—O(1^{iv})	2·84 (1)
Tl(1)—O(3^{viii})	3·49 (2)	Tl(2)—O(2)	2·96 (2)
Tl(1)—O(4^{vii})	2·98 (2)	Tl(2)—O(3^{viii})	3·16 (1)
Tl(1)—O(4)	2·99 (2)	Tl(2)—O(7)	3·22 (2)
Tl(1)—O(6^{vii})	3·05 (2)	Tl(2)—O(8^{v})	2·89 (2)
Tl(1)—O(10^{ix})	3·20 (2)	Tl(2)—O(9^{iv})	2·90 (2)
Tl(1)—O(10^{x})	3·03 (2)	Tl(2)—O(11^{iv})	3·55 (2)
Tl(1)—O(12^{x})	3·21 (2)		

Symmetry code: (i) $-x, \frac{1}{2}+y, \frac{1}{2}-z$; (ii) $1-x, 1-y, -z$; (iii) $1-x, 1-y, 1-z$; (iv) $x, \frac{1}{2}-y, z-\frac{1}{2}$; (v) $x, \frac{1}{2}-y, \frac{1}{2}+z$; (vi) $x-1, y, z$; (vii) $-x, -y, -z$; (viii) $x, y, z-1$; (ix) $x-1, \frac{1}{2}-y, z-\frac{1}{2}$; (x) $1-x, y-\frac{1}{2}, \frac{1}{2}-z$.

pound exhibits a more symmetrical space group ($P2_1/c$) identical to that of potassium, whereas the rubidium and caesium phases are characterized by the $P2_1$ group. This different behaviour of thallium compared to rubidium in spite of the similar size of these cations may be due to the presence of the $6s^2$ lone pair of Tl^+. Moreover, it is worth pointing out that one of the thallium ions [Tl(1)] is significantly displaced from the positions observed for potassium.

The Mo—O interatomic distances in the MoO_6 octahedra are characteristic of Mo^V with one abnormally short Mo—O bond, four intermediate Mo—O distances and a very long one (Table 2). The P(3)—O distances are close to those observed for a monophosphate, *i.e.* four almost equal distances. The P(1)—O and P(2)—O distances correspond to those observed in diphosphate groups, *i.e.* one long distance and three medium ones (Table 2). Tl(1) is surrounded by ten O atoms with Tl—O distances ranging from 2·98 (2) to 3·57 (2) Å and Tl(2) is linked to seven O atoms with $2{\cdot}84\,(1) < \mathrm{Tl—O} < 3{\cdot}55\,(2)$ Å (Table 2).

References

B. A. Frenz & Associates, Inc. (1982). *SDP Structure Determination Package*. College Station, Texas, USA.

Chen, J. J., Lii, K. M. & Wang, S. L. (1988). *J. Solid State Chem.* **76**, 204–209.

Costentin, G., Borel, M. M., Grandin, A., Leclaire, A. & Raveau, B. (1990). *J. Solid State Chem.* **89**, 31–38.

Haushalter, R. C. & Lai, F. W. (1989). *J. Solid State Chem.* **83**, 202–206.

Leclaire, A., Borel, M. M., Grandin, A. & Raveau, B. (1989). *Z. Kristallogr.* **188**, 77–83.

Leclaire, A., Borel, M. M., Grandin, A. & Raveau, B. (1990*a*). *Acta Cryst.* C**46**, 2009–2011.

Leclaire, A., Borel, M. M., Grandin, A. & Raveau, B. (1990*b*). *J. Solid State Chem.* **89**, 10–15.

Leclaire, A., Monier, J. C. & Raveau, B. (1983). *J. Solid State Chem.* **48**, 147–153.

Lii, K. M. & Haushalter, R. C. (1987). *J. Solid State Chem.* **69**, 320–328.

Lii, K. M., Johnston, D. C., Goshorn, D. P. & Haushalter, R. C. (1987). *J. Solid State Chem.* **71**, 131–138.

Riou, D. & Goreaud, M. (1989). *J. Solid State Chem.* **79**, 99–106.

Acta Cryst. (1991). C47, 1138–1141

$KVPO_5$, an Intersecting Tunnel Structure Closely Related to the Hexagonal Tungsten Bronze

By L. Benhamada, A. Grandin, M. M. Borel, A. Leclaire* and B. Raveau

Laboratoire de Cristallographie et Sciences des Matériaux, CRISMAT-ISMRa,
Boulevard du Maréchal Juin, 14050 *Caen CEDEX, France*

(*Received* 10 *June* 1990; *accepted* 18 *December* 1990)

Abstract. Potassium vanadium phosphate, M_r = 201·01, orthorhombic, $Pn2_1a$, a = 12·7640 (8), b = 10·5153 (9), c = 6·3648 (4) Å, V = 854·3 (2) Å^3, Z = 8, D_x = 3·13 Mg m^{-3}, λ/D(Mo $K\alpha$) = 0·71073 Å, μ = 2·94 mm^{-1}, $F(000)$ = 776, T = 294 K, R = 0·028, wR = 0·033 for 1321 independent reflections with $I >$

---

* To whom correspondence should be addressed.

0108-2701/91/061138-04$03.00

$3\sigma(I)$. The title compound is isostructural with $KTiPO_5$ described by Masse [Thesis (1974), Univ. of Grenoble, France]. Its mixed framework is built up from corner-sharing VO_6 octahedra and PO_4 tetrahedra delimiting tunnels where potassium cations are located. A new description of the structure is proposed. The host lattice VPO_5 is built from infinite chains of octahedra $[VO_3]_\infty$, belonging to the hexagonal tungsten bronze structure, running along [011] and [01$\bar{1}$]. Connection between the octahedral chains is ensured by single PO_4 tetrahedra.

Introduction. The association of MO_6 octahedra of transition elements with PO_4 tetrahedra allows a great number of tunnel structures to be built, whose host lattices are often closely related to those of pure octahedral structures. This is true for instance in the cases of the tungsten and niobium phosphate bronzes (Borel, Goreaud, Grandin, Labbe, Leclaire & Raveau, 1991), which are derived from perovskite, tetragonal tungsten bronzes and hexagonal tungsten bronzes (Magneli, 1949, 1953). In this respect, vanadium seems to exhibit a different behaviour. Although the two vanadium phosphates $K_2V_3P_4O_{17}$ (Leclaire, Chahboun, Groult & Raveau, 1988) and $Cs_2V_3P_4O_{17}$ (Lii & Wang, 1989) possess a tunnel structure, they do not show close relationships with pure octahedral oxides. During investigation of the system K–V–P–O, a new vanadium(IV) phosphate, $KVPO_5$, was isolated, which we found to be isostructural with the phosphate $KTiPO_5$ described by Masse (1974). The present paper deals with the structure of this phase and with the study of its relationships with the hexagonal tungsten bronze (HTB).

Experimental. Dark blue crystals of $KVPO_5$ crystallized as a minor product in a mixture of composition '$K_7V_8P_9O_{44}$' in the following way: firstly a mixture of $H(NH_4)_2PO_4$, V_2O_5 and K_2CO_3 in appropriate ratios was heated in a platinum crucible for 2 h at 653 K to decompose the phosphate and carbonate; secondly the appropriate amount of vanadium was added. The product was grown and heated in an evacuated silica ampoule for 7 d at 923 K. Crystal 0·084 × 0·072 × 0·048 mm. Enraf–Nonius CAD-4 diffractometer. Unit cell: least squares on 25 reflections, $\pm 2\theta$, $18 < 2\theta < 22°$. Intensity measurement by ω–θ of $(1 + 0{\cdot}35\tan\theta)°$ scan, and $(1 + \tan\theta)$ mm counter aperture slit determined by a study of some reflections in the ω–θ plane. Scanning speed adjusted to obtain $\sigma(I)/I < 0{\cdot}018$ or to approach it in a time limited to 60 s. Three standards for count every 3000 s; no appreciable trends. $0 \leq \theta \leq 45°$; $0 \leq h \leq 15$, $0 \leq k \leq 20$, $-12 \leq l \leq 0$. 3181 reflections measured, 1321 with $I/\sigma(I) \geq 3$ used to solve and refine the structure. No correction made for extinction or absorption. Structure solved by heavy-atom methods. Refinement on F. All subsequent calculations on a MicroVAXII with the *SDP* system (B. A. Frentz & Associates, Inc., 1982); all atoms refined anisotropically. Atomic scattering factors from *International Tables for X-ray Crystallography* (1974, Vol. IV), $(\Delta/\sigma)_{max} = 0{\cdot}005$, $\Delta\rho < 0{\cdot}7$ e Å^{-3}, $R = 0{\cdot}028$, $wR = 0{\cdot}033$, $w = f(\sin\theta/\lambda)$. Atomic parameters in Table 1,* bond distances and angles in Table 2.

Table 1. *Positional parameters with e.s.d.'s in parentheses*

	x	y	z	B(Å^2)
V(1)	0·12417 (5)	0·250	−0·0038 (1)	0·326 (8)
V(2)	0·24842 (7)	0·49719 (9)	0·2750 (1)	0·328 (8)
P(1)	0·18046 (9)	0·2337 (1)	0·4976 (2)	0·38 (1)
P(2)	−0·0028 (1)	0·4879 (1)	0·1681 (2)	0·33 (1)
K(1)	0·3806 (1)	0·4332 (1)	0·7812 (2)	1·54 (2)
K(2)	0·3971 (1)	0·1794 (2)	0·2057 (2)	1·46 (2)
O(1)	0·1119 (3)	0·2051 (3)	0·3054 (5)	0·62 (5)
O(2)	0·1104 (3)	0·2622 (4)	−0·3134 (5)	0·70 (5)
O(3)	0·0092 (3)	0·3683 (3)	0·0278 (6)	0·59 (6)
O(4)	0·0182 (3)	0·1021 (4)	−0·0232 (6)	0·76 (6)
O(5)	0·2272 (3)	0·1032 (4)	−0·0395 (6)	0·63 (6)
O(6)	0·2202 (3)	0·3538 (4)	0·0334 (6)	0·73 (6)
O(7)	0·3991 (3)	0·4666 (3)	0·1950 (5)	0·53 (5)
O(8)	0·2474 (3)	0·6177 (3)	0·0373 (5)	0·59 (5)
O(9)	0·0931 (3)	0·5047 (4)	0·3109 (5)	0·62 (5)
O(10)	0·2557 (3)	0·3449 (3)	0·4521 (6)	0·68 (5)

Anisotropically refined atoms are given in the form of the isotropic equivalent displacement parameter defined as: $(4/3)[a^2B(1,1) + b^2B(2,2) + c^2B(3,3) + ab(\cos\gamma)B(1,2) + ac(\cos\beta)B(1,3) + bc(\cos\alpha)B(2,3)]$.

Discussion. The 'VPO_5' framework is built up from corner-sharing VO_6 octahedra and PO_4 tetrahedra (Figs. 1 and 2). One observes $[VPO_8]_\infty$ chains where one octahedron alternates with one tetrahedron. Half of these chains run along **a** and half of them run along **c**. Two chains running along **c** are linked *via* a chain running along **a** and *vice versa*.

Each PO_4 shares its corners with four VO_6 octahedra whereas each VO_6 octahedron shares its corners with four PO_4 tetrahedra and two VO_6 octahedra.

This framework delimits two sorts of six-sided tunnels running along **a** and **c**, respectively. The first type of tunnel (Fig. 1) is formed of rings of four VO_6 octahedra sharing their corners with two PO_4 tetrahedra, whereas the second type of tunnel (Fig. 2), which exhibits rings of three VO_6 octahedra sharing their corners with three PO_4 tetrahedra, is very similar to those observed in the hexagonal tungsten bronze structure (HTB) described by Magneli (1953). In fact the projection of the structure onto (100) (Fig. 1) shows the existence of infinite $[VO_3]_\infty$ chains

---

* Lists of structure factors and anisotropic thermal parameters have been deposited with the British Library Document Supply Centre as Supplementary Publication No. SUP 53849 (10 pp.). Copies may be obtained through The Technical Editor, International Union of Crystallography, 5 Abbey Square, Chester CH1 2HU, England.

Table 2. *Distances* (Å) *and angles* (°) *in the* VO_6 *and* PO_4 *polyhedra and main K—O distances*

The V—O(*i*) or P—O(*i*) distances are on the diagonal, above it are the O(*i*)—O(*j*) distances, and under it are the O(*i*)—V—O(*j*) angles.

V(1)	O(1)	O(2)	O(3)	O(4)	O(5)	O(6)
O(1)	2·030 (4)	3·984 (5)	2·7901 (6)	2·642 (6)	2·852 (6)	2·712 (6)
O(2)	166·39 (2)	1·982 (4)	2·762 (6)	2·763 (6)	2·838 (6)	2·786 (6)
O(3)	89·43 (2)	89·69 (2)	1·934 (4)	2·821 (5)	3·962 (7)	2·697 (7)
O(4)	80·33 (2)	86·08 (2)	89·64 (2)	2·065 (4)	2·670 (7)	3·713 (7)
O(5)	88·96 (2)	89·73 (2)	170·76 (2)	81·12 (2)	2·040 (4)	2·678 (6)
O(6)	94·12 (2)	99·47 (2)	97·02 (2)	171·32 (2)	92·17 (2)	1·658 (4)

V(2)	$O(5^{\mathrm{I}})$	O(6)	O(7)	O(8)	O(9)	O(10)
$O(5^{\mathrm{i}})$	1·653 (4)	3·836 (6)	2·741 (6)	2·717 (6)	2·691 (6)	2·725 (6)
O(6)	178·27 (2)	2·183 (5)	2·771 (6)	2·797 (6)	2·875 (6)	2·705 (7)
O(7)	96·21 (2)	82·50 (2)	2·015 (4)	2·698 (6)	3·995 (5)	2·769 (6)
O(8)	96·65 (2)	84·40 (2)	85·13 (2)	1·973 (4)	2·885 (6)	3·900 (5)
O(9)	94·50 (2)	86·80 (2)	169·28 (2)	93·20 (2)	1·997 (4)	2·817 (7)
O(10)	97·52 (2)	81·31 (2)	88·28 (2)	164·94 (2)	90·76 (2)	1·960 (4)

P(1)	O(1)	O(2)	$O(8^{\mathrm{ii}})$	O(10)
O(1)	1·534 (4)	2·500 (5)	2·500 (6)	2·530 (6)
O(2)	109·42 (2)	1·528 (4)	2·550 (6)	2·534 (6)
$O(8^{\mathrm{ii}})$	108·39 (2)	111·96 (2)	1·548 (4)	2·450 (5)
O(10)	110·74 (2)	111·29 (2)	104·94 (2)	1·541 (4)

P(2)	O(3)	$O(4^{\mathrm{iii}})$	$O(7^{\mathrm{iv}})$	O(9)
O(3)	1·550 (4)	2·483 (5)	2·482 (6)	2·540 (6)
$O(4^{\mathrm{iii}})$	107·60 (2)	1·526 (5)	2·522 (6)	2·534 (6)
$O(7^{\mathrm{iv}})$	106·75 (2)	110·57 (3)	1·541 (4)	2·509 (5)
O(9)	110·82 (3)	111·73 (3)	109·26 (2)	1·534 (4)

K(1)—$O(1^{\mathrm{i}})$	2·865 (4)	K(2)—$O(3^{\mathrm{v}})$	2·798 (5)
K(1)—$O(3^{\mathrm{v}})$	2·651 (5)	K(2)—$O(4^{\mathrm{v}})$	2·670 (5)
K(1)—$O(4^{\mathrm{i}})$	2·928 (5)	K(2)—O(5)	2·790 (5)
K(1)—$O(5^{\mathrm{i}})$	3·042 (5)	K(2)—O(6)	3·109 (5)
K(1)—O(6)	2·732 (5)	K(2)—O(7)	3·021 (4)
K(1)—O(7)	2·668 (4)	K(2)—$O(8^{\mathrm{ii}})$	2·877 (5)
K(1)—O(8)	3·052 (5)	K(2)—$O(9^{\mathrm{vi}})$	3·115 (4)
K(1)—O(10)	2·791 (5)	K(2)—O(10)	2·958 (5)
K(2)—$O(1^{\mathrm{v}})$	2·755 (5)		

Symmetry codes: (i) $\frac{1}{2}-x,\ \frac{1}{2}+y,\ \frac{1}{2}+z$; (ii) $\frac{1}{2}-x,\ -\frac{1}{2}+y,\ \frac{1}{2}+z$; (iii) $\frac{1}{2}-x,\ \frac{1}{2}+y,\ -z$; (iv) $-\frac{1}{2}+x,\ y,\ \frac{1}{2}-z$; (v) $\frac{1}{2}+x,\ y,\ \frac{1}{2}-z$; (vi) $\frac{1}{2}-x,\ -\frac{1}{2}+y,\ -\frac{1}{2}+z$.

of corner-sharing octahedra running along the [011] and $[01\bar{1}]$ directions. The great similarity of this structure with HTB's is better seen by considering one layer of polyhedra parallel to (011) (Fig. 2). Such a layer is indeed built up from HTB-$[VO_3]_\infty$ chains running along $[01\bar{1}]$ linked *via* single PO_4 tetrahedra and *via* $[VPO_8]_\infty$ chains. The VO_6 octahedra of the VPO_8 chains in fact belong to HTB-$[VO_3]_\infty$ chains, which run along the [011] direction in a layer of polyhedra parallel to $(01\bar{1})$; the geometry of the latter is absolutely identical to that of the (011) layer. Moreover, two successive $[VO_3]_\infty$ chains are linked *via* single PO_4 tetrahedra in the direction orthogonal to the (011) or $(01\bar{1})$ plane. Thus the $[VPO_5]_\infty$ framework can be described as the assemblage of infinite $[VO_3]_\infty$ HTB chains linked *via* single PO_4 tetrahedra. Along **c**, two successive chains are parallel, *i.e.* both parallel to [011] or to $[01\bar{1}]$ (Fig. 1), whereas along **a** the successive $[VO_3]_\infty$ chains are parallel to $[01\bar{1}]$ alternately.

The PO_4 tetrahedra have the classical geometry observed for monophosphates, with four almost equal distances (Table 2). The VO_6 octahedra are characterized by one abnormally short V—O bond (1·65 Å), four intermediate V—O bonds (1·93 to 2·06 Å) which correspond generally to the oxygens linked to phosphorus, and one longer V—O bond (2·04–2·18 Å). It is worth pointing out that in the $[VO_3]_\infty$ HTB chains, the short V—O bond alternates

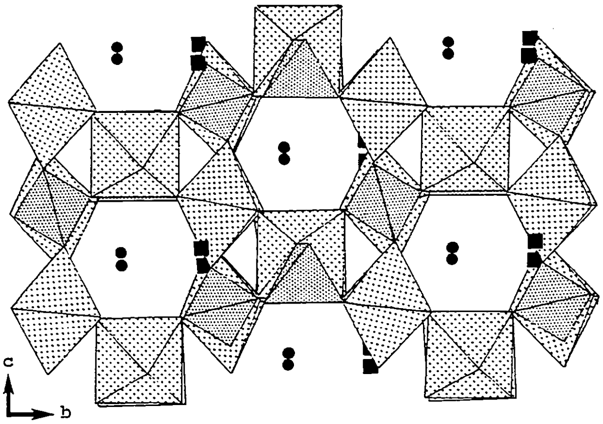

Fig. 1. Projection of the structure along **a**.

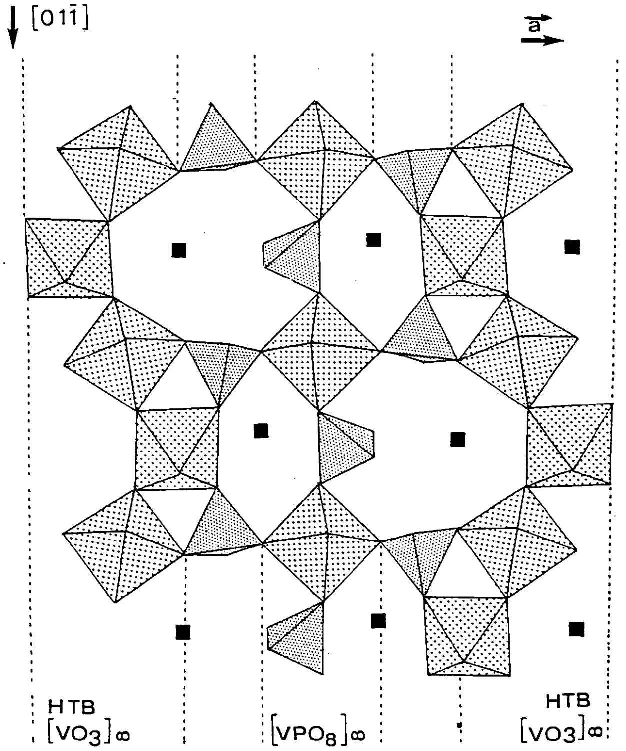

Fig. 2. The (011) layer built up of HTB-$[VO_3]_\infty$ chains and $[VPO_8]_\infty$ chains linked one to the other by PO_4 tetrahedra.

with a long one as in $K_2V_3P_4O_{17}$ (Leclaire *et al.*, 1988). Moreover it must also be emphasized that the apex corresponding to the shortest V—O bond is not free, contrary to the Mo^V phosphates, which are always described as molybdenyl compounds.

The d^1 configuration of V^{IV} suggests the possibility of particular electron transport properties due to the one-dimensional character of $[VO_3]_\infty$ chains. In the same way, the existence of intersecting tunnels indicates possible mobility of the K^+ cations, leading to ion exchange properties and ionic conductivity.

References

B. A. Frenz & Associates, Inc. (1982). *SDP Structure Determination Package*. College Station, Texas, USA.
Borel, M. M., Goreaud, M., Grandin, A., Labbe, Ph., Leclaire, A. & Raveau, B. (1991). *Eur. J. Solid State Inorg. Chem.* **28**, 93–129.
Leclaire, A., Chahboun, A., Groult, D. & Raveau, B. (1988). *J. Solid State Chem.* **77**, 170–179.
Lii, K. H. & Wang, Y. P. (1989). *J. Solid State Chem.* **80**, 127–132.
Magneli, A. (1949). *Arkiv. Chem.* **1**, 213–269.
Magneli, A. (1953). *Acta Chem. Scand.* **7**, 315–319.
Masse, R. (1974). Thesis, Univ. of Grenoble, France.

Acta Cryst. (1991). C**47**, 1141–1143

Structure of Sb_2Te

By V. Agafonov and N. Rodier

Laboratoire de Chimie Minérale et de Cristallographie, Faculté de Pharmacie, 5 rue J.-B. Clément, 92296 Châtenay-Malabry CEDEX, France

R. Céolin

Laboratoire de Chimie Physique, Faculté de Pharmacie, 2 bis Boulevard Tonnelé, 37042 Tours CEDEX, France

R. Bellissent

Laboratoire Léon Brillouin, CEA-CNRS, CEN-Saclay, 91191 Gif sur Yvette CEDEX, France

C. Bergman

CTM du CNRS, 26 avenue du 141ème RIA, 13003 Marseille, France

and J. P. Gaspard

Institut de Physique, Université de Liège, B-4000 Sart Tilman, Belgique

(*Received* 1 *August* 1990; *accepted* 26 *November* 1990)

Abstract. Diantimony–tellurium, Sb_2Te, $M_r = 371{\cdot}1$, trigonal, $P\bar{3}m1$, $a = 4{\cdot}272$ (1), $c = 17{\cdot}633$ (3) Å, $V = 278{\cdot}6$ (2) Å^3, $Z = 3$, $D_x = 6{\cdot}63$ Mg m^{-3}, $\lambda(\text{Mo } K\bar{\alpha}) = 0{\cdot}7107$ Å, $\mu = 22{\cdot}11$ mm^{-1}, $F(000) = 462$, $T = 294$ K, final $R = 0{\cdot}035$ for 245 independent observed reflections. The structure of Sb_2Te consists of nine layers stacked along the *c* axis and presents the combination of five-layer stacks of Sb_2Te_3 and two-layer stacks of Sb_2.

Introduction. The layered compounds of the Sb—Te system, such as Sb_2Te_3, SbTe and Sb_2Te, are important for industrial applications owing to the strong anisotropy in their electronic properties. These compounds, as well as the phases of the Bi–Te and Bi–Se systems, have trigonal or rhombohedral symmetries with a similar *a* parameter while the *c* parameter depends on the number of layers, which is itself connected to the chemical composition (Imamov & Semiletov, 1971). The crystal structures of Sb_2Te_3 (Semiletov, 1956; Anderson & Krause, 1974) and SbTe (Stasova & Karpinskii, 1967) are already known. In this paper, the results of the Sb_2Te crystal structure determination are reported.

Experimental. Single crystals of Sb_2Te were obtained by slow cooling a molten stoichiometric (2:1) mixture of Sb and Te. A platelet-like crystal (0·38 × 0·07 × 0·02 mm) with well defined faces was chosen. Enraf–Nonius CAD-4 diffractometer; lattice parameters determined from 25 reflections having $8{\cdot}87° \le \theta \le 19{\cdot}87°$, θ–2θ scan technique; $0{\cdot}049 \le (\sin\theta)/\lambda \le$

0108-2701/91/061141-03$03.00